Apply Complex Source Beam Technique for Effective NF-FF Transformations

Shih-Chung Tuan [1], Hsi-Tseng Chou[2] and Prabhakar H.Pathak[3]
1. Dept. of Communication. Eng., Oriental Institute of Technology, Taiwan
2. Dept. of Communication Eng., Yuan Ze University, Taiwan
3. Dept. of Electrical and Computer Eng., Ohio State University, USA

***Abstract*- This paper presents a general technique for an effective near-field to far-field transformation based on the complex source beam (CSB) method. In this technique, a set of CSBs launched from the center of antenna under test is used to represent the antenna's radiation. The weightings of CSBs are found by matching the near-fields measured on a pre-described surface in the conventional measurement systems. All three conventional measurement techniques including planar, cylindrical and spherical measurement systems are examined to validate the CSB method with accuracy comparisons in the near- and far-field patterns.**

I. INTRODUCTION

Near-field (NF) measurement systems are widely used to measure the antenna's radiation characteristics. Depending on the natures of antennas in terms of their radiation directivities, various system configurations have been developed to provide effective measurements of antenna radiations at the development stages. Three typical and most widely used ones are the planar, cylindrical and spherical near-field measurement systems, which measure the radiation fields on the planar, cylindrical and spherical surfaces, respectively enclosing the antennas under test (AUT). In order to obtain the far-field(FF) radiation characteristics, which are most commonly used to justify the antenna characteristics in the antenna community, the near-field to far-field(NF-FF) transformations need to be performed using the measured near-field information on the respective surfaces. In the past, NF-FF transformation techniques are developed and performed according to the natures of system configurations. For example, a fast Fourier transformation (FFT) scheme can be used to efficiently obtain the far-field radiations of highly directive antennas, such as reflector antennas, in the planar near-field measurement system. On the other hand, cylindrical and spherical wave type expansions have also been used in the literatures for the cylindrical and spherical system. There are several drawbacks in those transformation techniques. First, those transformation techniques are relatively independent in their natures, and do not share common characteristics in the expansions. Second, those techniques experience different degrees of truncation diffraction effects in the transformation procedures. Several studies and techniques have been reported in the literatures to discuss the truncation errors and reduce these effects based on the numerical method of moment (MoM), which increases the computational complexity. Third, the utilization of measured data has been limited in these conventional transformation techniques. Those drawbacks have significantly limited the applications of NF measurement systems.

This paper presents an effective approach to alternatively resolve the above mentioned shortcomings based on the applications of complex source beam (CSB) techniques[1,2,4]. In particular, a set of CSBs are selected to serve as field basis functions launched radially from the center of AUT. The measured NF data on the selected surface boundaries is represented in terms of this CSB set. The advantages of this CSB technique, responding to each of the above mentioned shortcoming, are apparent due to a fact that the CSB is a solution of Maxwell's equations. First, this CSB technique can be applied universally to a NF measurement system with a relatively arbitrary scan surface including the conventional three NF systems mentioned in the previous paragraphs, which are examined in this paper to validate the technique. Secondly, each CSB function is continuous in the spatial extent. The superposition of CSBs after the NF expansion provides a continuous field variation along the selected surface of measurement system. The truncation errors due to the existence of measurement surface boundaries can be reduced without the need to impose additional taper functions. Third, after the expansion each of the CSB functions can be treated independently, and can be used in conjunction with other simulation techniques to justify AUT's characteristics when it is used in a realistic practice. For example, in [3] CSB techniques have been developed to efficiently analyze the reflector antenna when it is illuminated by the radiation of a feed antenna.

II. CHARACTERISTIC OF CSB FIELDS

The CSB is an electromagnetic field radiated from a current source located in a complex space. This section reviews the near- and far-field formulations to exhibit the characteristics of field variations from a near-zone to far zone, which makes the NF to FF transformation in a nature of wave propagation. the CSB can be formulated as

$$\overline{E}_{m,e}(\overline{r}) = \frac{jk}{4\pi}\begin{Bmatrix} Z_0\hat{R}\times\hat{R}\times d\overline{p}_e \\ \hat{R}\times d\overline{p}_m \end{Bmatrix}\int \frac{e^{kb}e^{-jkz\left(1+\frac{x^2+y^2}{2(z^2+b^2)}\right)}e^{-\frac{kb}{2}\left(\frac{x^2+y^2}{z^2+b^2}\right)}}{z+jb}. \qquad (1)$$

the formulation in (1) clearly shows a Gaussian field distribution in the direction (x-y plane) transverse to the beam axis ($\hat{z}$).The CSB field in the far zone of beam waist can be formulated by using the following approximation:

$$\overline{E}_{m,e}(\bar{r}) = \frac{jk}{4\pi}\begin{Bmatrix} Z_0\hat{r}\times\hat{r}\times d\bar{p}_e \\ \hat{r}\times d\bar{p}_m \end{Bmatrix}\frac{1}{r}e^{-jkr}e^{jk\bar{r}_o\bullet\hat{r}}e^{kb\hat{b}\bullet\hat{r}} \tag{2}$$

In this section, the strategies to represent the radiations of antenna under test (AUT) by a set of CSBs are described. The procedure to obtain the CSBs' weightings by matching its field values with the measured data on the measurement surface is also developed. Once the weightings are found, the CSBs can be ready and used to find the far field radiation. Figure1. shows the discretized grids of CSBs' axes on the virtual spherical surface, S_{dis} , enclosing the AUT. Figure2., where a measurement surface, S_m , is assumed to measure the NF data. It is noted that S_m enclosing AUT can be relatively arbitrary, and are planar, cylindrical and spherical for the three conventional NF measurement systems. Assuming electrical current sources, the CSB representation of AUT's radiation can be generally expressed as

$$\overline{E}_{AUT}(r) = \sum_{n=1}^{N}\left(A_n\overline{G}_n^1(\bar{r}) + B_n\overline{G}_n^2(\bar{r})\right) \tag{3}$$

Where

$$\begin{bmatrix}\overline{G}_n^1(\bar{r}) \\ \overline{G}_n^2(\bar{r})\end{bmatrix} = e^{-kb}\frac{jk}{4\pi}Z_0\hat{R}_n\times\hat{R}_n\times\begin{bmatrix}\hat{u}_{1,n} \\ \hat{u}_{2,n}\end{bmatrix}\frac{e^{-jkR_n}}{R_n} \tag{4}$$

$$\begin{cases} E_{1,p}^{mea} = \sum_{n=1}^{N}\left[A_n\left(\overline{G}_n^1(\bar{r}_p^m)\cdot\hat{u}_{1,p}\right) + B_n\left(\overline{G}_n^2(\bar{r}_p^m)\cdot\hat{u}_{1,p}\right)\right] \\ E_{2,p}^{mea} = \sum_{n=1}^{N}\left[A_n\left(\overline{G}_n^1(\bar{r}_p^m)\cdot\hat{u}_{2,p}\right) + B_n\left(\overline{G}_n^2(\bar{r}_p^m)\cdot\hat{u}_{2,p}\right)\right] \end{cases} \tag{5}$$

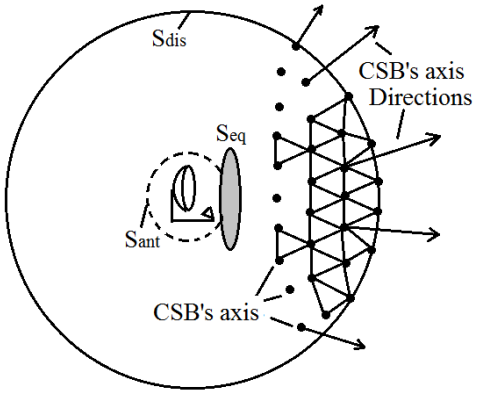

Figure 1: Illustration of CSB discretization grids to launch the axes of CSBs. The relation to AUT's size to justify the resolution of CSB grids is also shown.

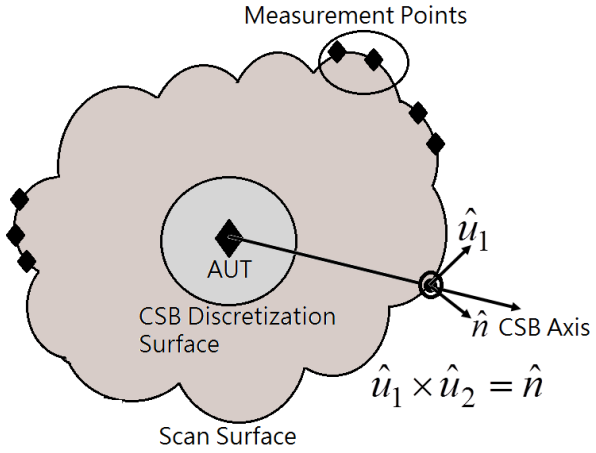

Figure 2: Applications of CSB technique to represent AUT's radiation and the relationship to the measurement surface.

. A minimum least square error scheme can be used to solve (5) for (A_n, B_n) $n=1\sim N$, which can be achieved via a simple MATLAB command by

$$[D] = [G]\backslash[E], \tag{6}$$

where

$$[D] = \begin{bmatrix} A_n \\ \vdots \\ B_n \\ \vdots \end{bmatrix}_{2N\times 1}; \qquad [E] = \begin{bmatrix} E_{1,p}^{mea} \\ \vdots \\ E_{2,p}^{mea} \\ \vdots \end{bmatrix}_{2M\times 1} \tag{7a);(7b)}$$

and

$$[G] = \begin{bmatrix} \overline{G}_n^1(\bar{r}_p^m)\cdot\hat{u}_{1,p} & \cdots & \overline{G}_n^2(\bar{r}_p^m)\cdot\hat{u}_{1,p} & \cdots \\ \vdots & \ddots & \vdots & \vdots \\ \overline{G}_n^1(\bar{r}_p^m)\cdot\hat{u}_{2,p} & \cdots & \overline{G}_n^2(\bar{r}_p^m)\cdot\hat{u}_{2,p} & \cdots \\ \vdots & \ddots & \vdots & \vdots \end{bmatrix}. \tag{8}$$

In the practical implementation, most of the computation time is used to compute (8), which however needs to be computed only once regardless of any AUT, This matrix can be stored in advance once the system setup has been established. Once these coefficients are found, (2) can be used to find the far-field of AUT.

III. Numerical Examples

The CSB technique is validated by its treatments of NF-FF transformations for the three conventional measurement systems, which include planar, cylindrical and spherical near-field measurement systems. In particular, the NSI systems (modeled by NSI 300V series Planar/cylindrical NF Antenna Measurement System and NSI-700S-90 Spherical NF Antenna Measurement System, respectively for the three systems) are used to measure the radiations of a standard gain horn-type antenna, SGH430 at a frequency of 2.45GHz, which has been widely used as a reference of antenna's gain comparison. The validations on NF representations and far-field patterns are examined and shown in the following.

A. *Planar Near-Field Measurement*

Figure3. It shows Implementation of CSB technique in the planar near-field measurement system. Figure4. It shows the comparison of radiation patterns between CSB synthesized and measured data, respectively. On Figure 4(a) and (b), the FF data was taken on the two principal planes ($\phi = 0^o$ and $\phi = 90^o$), respectively.

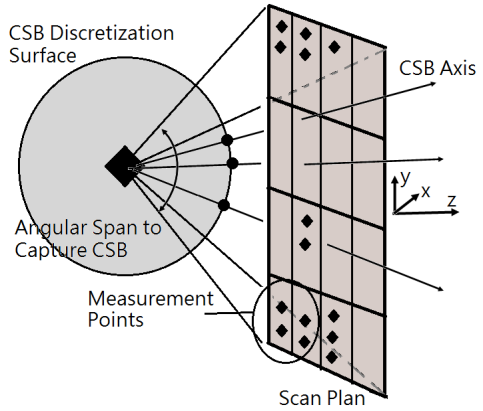

Figure 3: Implementation of CSB technique in the planar near-field measurement system.

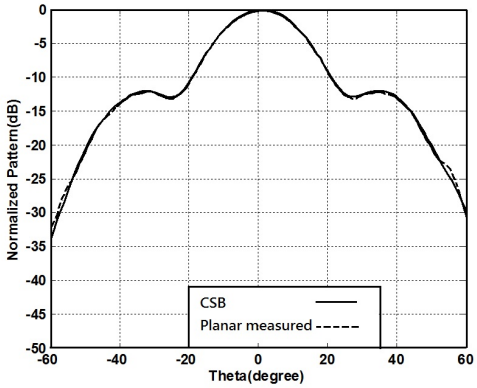

Figure 4(a) The FF data was taken on the E-planes

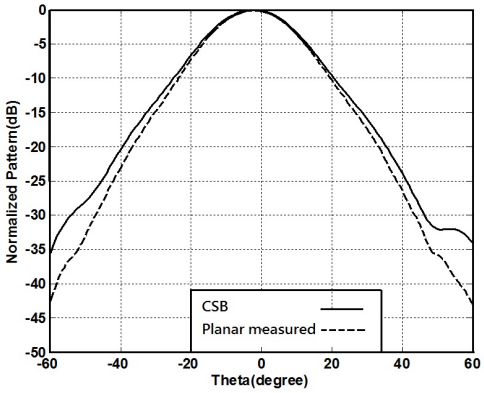

Figure 4(b) The FF data was taken on the H-planes

B. Cylindrical Near-Field Measurement

Figure5. It shows Implementation of CSB technique in the cylindrical near-field measurement system. On Figure 6 (a) and (b) the FF data was taken on the two principal planes ($\phi = 0^o$ and $\phi = 90^o$), respectively.

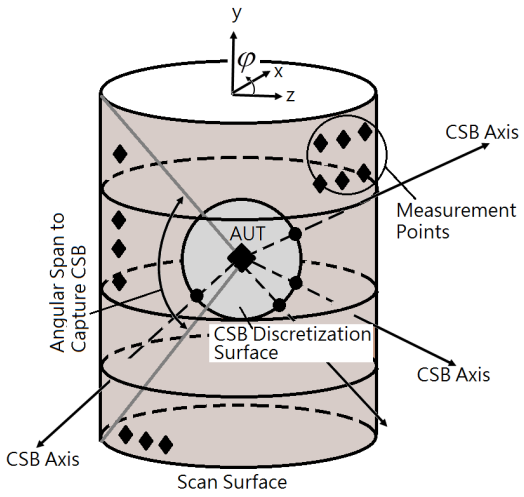

Figure 5: Implementation of CSB technique in the cylindrical near-field measurement system.

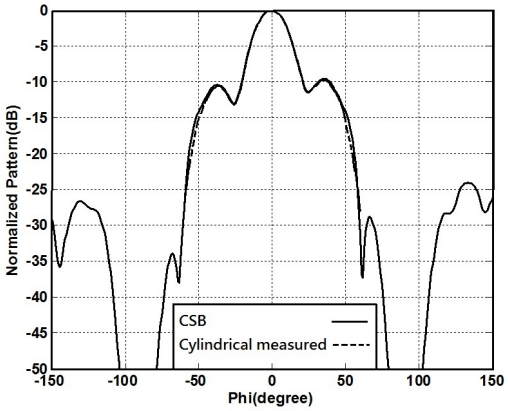

Figure 6(a) The FF data was taken on the E-planes

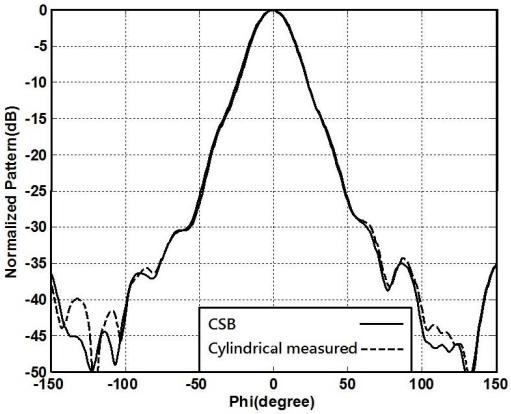

Figure 6(b) The FF data was taken on the H-planes

C. SPHERICAL NEAR-FIELD MEASUREMENT

Figure7. It shows Implementation of CSB technique in the spherical near-field measurement system. On Figure 8 (a) and (b) the FF data was taken on the two principal planes ($\phi = 0^o$ and $\phi = 90^o$), respectively.

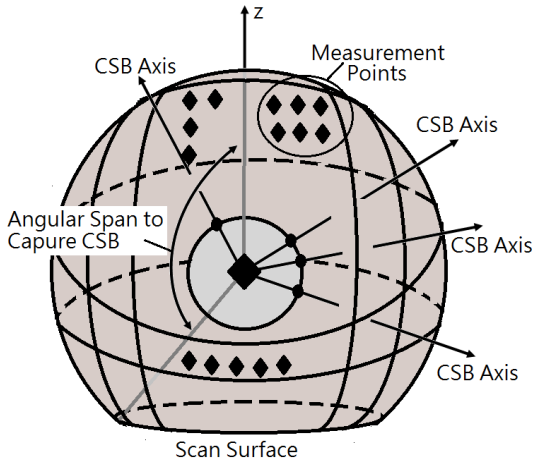

Figure 7: Implementation of CSB technique in the spherical near-field measurement system.

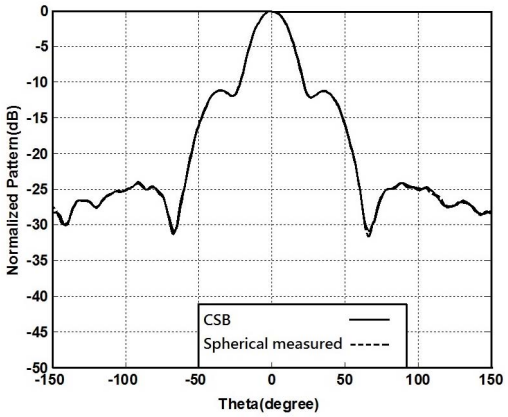

Figure 8(a) The FF data was taken on the E-planes

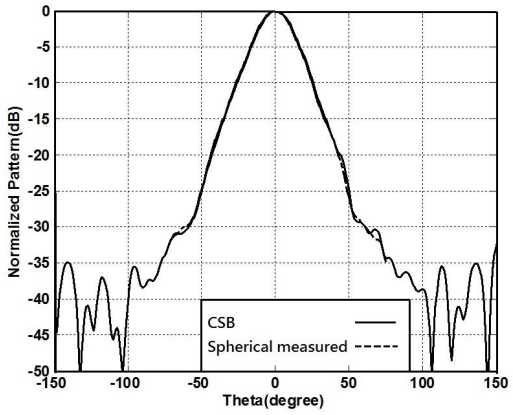

Figure 8(b) The FF data was taken on the H-planes

IV. CONCLUSIONS

This paper presents an effective approach to alternatively resolve the above mentioned shortcomings based on the applications of complex source beam (CSB) techniques. In this technique, a set of CSBs launched from the center of antenna under test is used to represent the antenna's radiation. The weightings of CSBs are found by matching the near-fields measured on a pre-described surface in the conventional measurement systems.

REFERENCES

[1] J.B Keller and W. Streifer, "Complex Rays with an Application to Gaussian Beam" J. Opt. Soc. Amer., vol.61,pp.40-43,1971.

[2] G.A Deschamps, "Gaussian Beam as a Bundle of Complex Rays" Electronics Letters, vol.7, pp.684-685,Nov, 1971.

[3] H-T Chou, Shih-Chung Tuan, H-H Chou " Transient Analysis of Scattering From a Perfectly Conducting Parabolic Reflector Illuminated by a Gaussian Beam Electromagnetic Field" *IEEE Transactions on Antennas and Propagation, Vol. 58, No.5, pp.1711~1719, May 2010.*

[4] George C. Zogbi " Reflection and Diffraction of General Astigmatic Gaussian Beams From Curved Surfaces and Edges," Ph.D. Dissertation, The Ohio State University, June 1994.